The oxidative addition of cyanogen bromide to *C,N*-chelated and Lappert's Stannylenes

Petr Švec[a*], Maksim A. Samsonov,[a] Zdeňka Růžičková,[a] Jiří Brus,[b] Aleš Růžička[a]

[a]Department of General and Inorganic Chemistry, Faculty of Chemical Technology, University of Pardubice, Studentská 573, CZ-532 10, Pardubice, Czech Republic
[b]Institute of Macromolecular Chemistry CAS, Heyrovského nám. 2, CZ-162 06, Prague, Czech Republic
**Corresponding author, e-mail: petr.svec2@upce.cz*

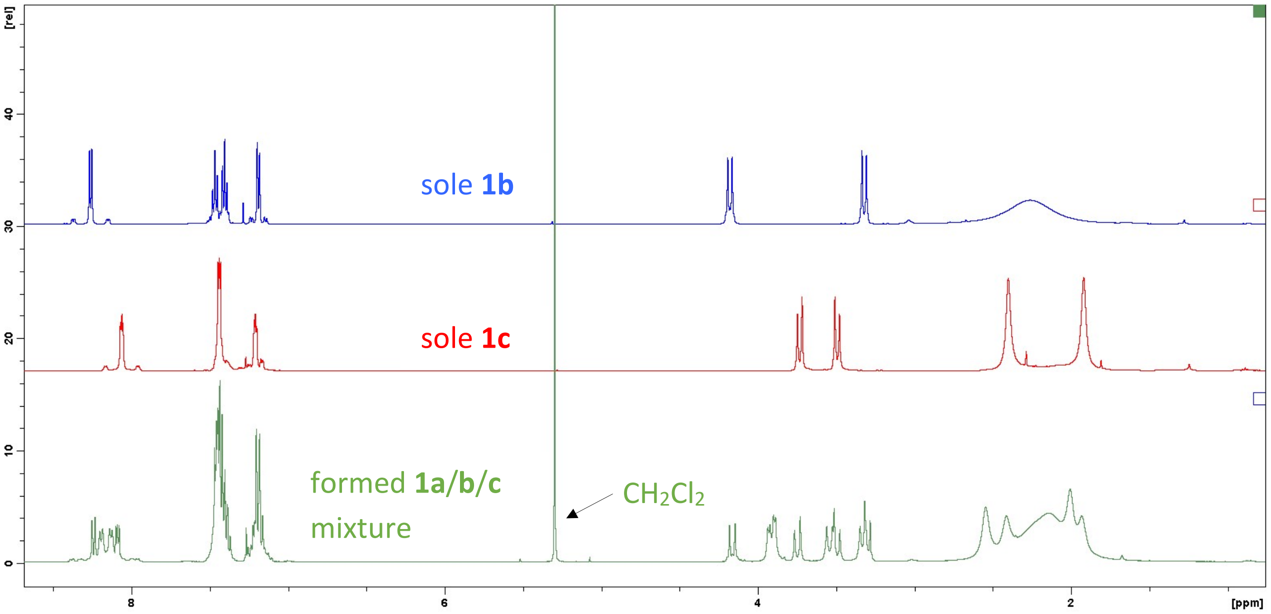

Fig. S1: ^{1}H NMR spectra of sole **1b** (blue), **1c** (red) and **1a/b/c** mixture formed *via* the reaction of **1** with BrCN (green) measured in $CDCl_3$. The resonance at 5.30 ppm in the bottom green spectrum is due to the presence of the CH_2Cl_2 solvent.

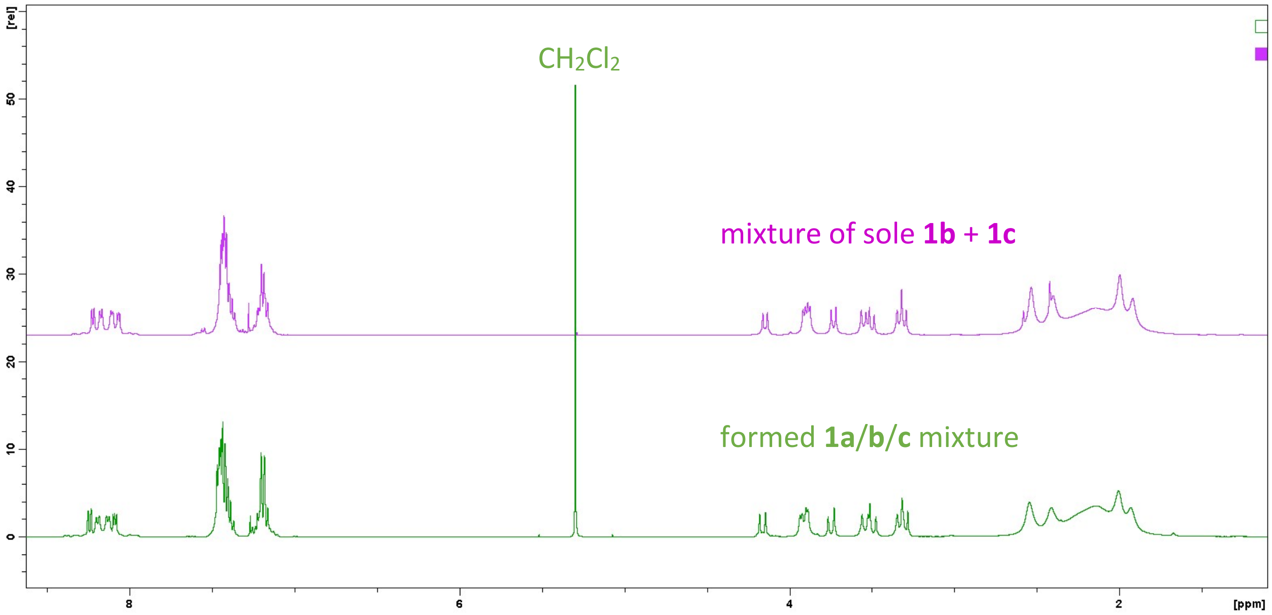

Fig. S2: ^{1}H NMR spectra of mixture of sole **1b** + **1c** (violet) and **1a/b/c** mixture formed *via* the reaction of **1** with BrCN (green) in $CDCl_3$. The resonance at 5.30 ppm in the bottom green spectrum is due to the presence of the CH_2Cl_2 solvent.

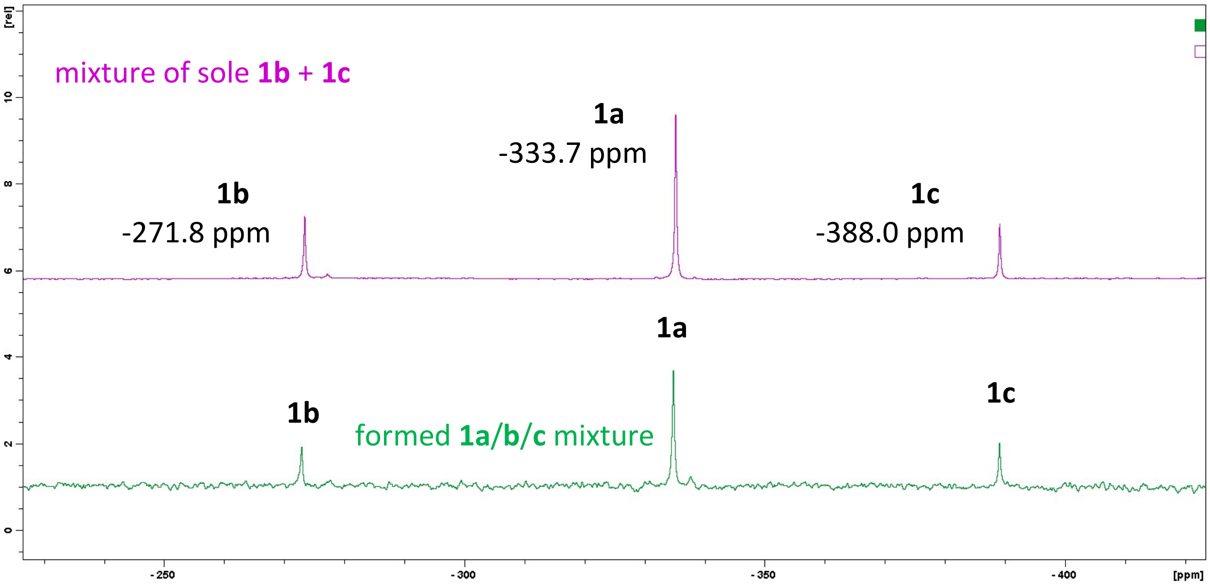

Fig. S3: ^{119}Sn NMR spectra of mixture of sole **1b** + **1c** (violet) and **1a/b/c** mixture formed *via* the reaction of **1** with BrCN (green) in $CDCl_3$.

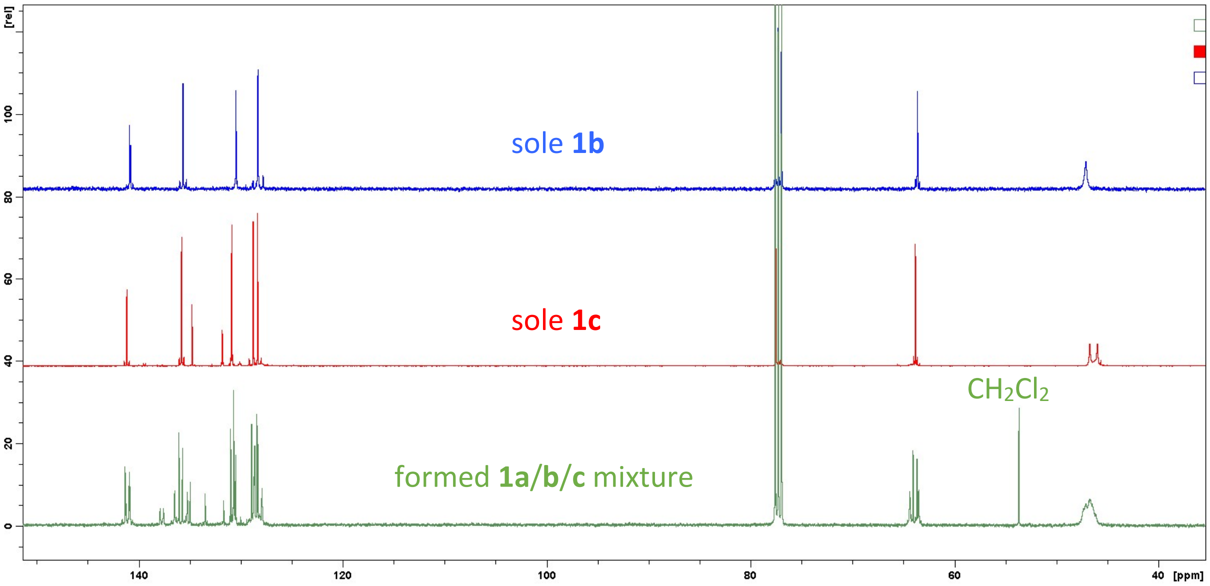

Fig. S4: ^{13}C NMR spectra of sole **1b** (blue), **1c** (red) and **1a/b/c** mixture formed *via* the reaction of **1** with BrCN (green) measured in $CDCl_3$. The resonance at 53.6 ppm in the bottom green spectrum is due to the presence of the CH_2Cl_2 solvent.

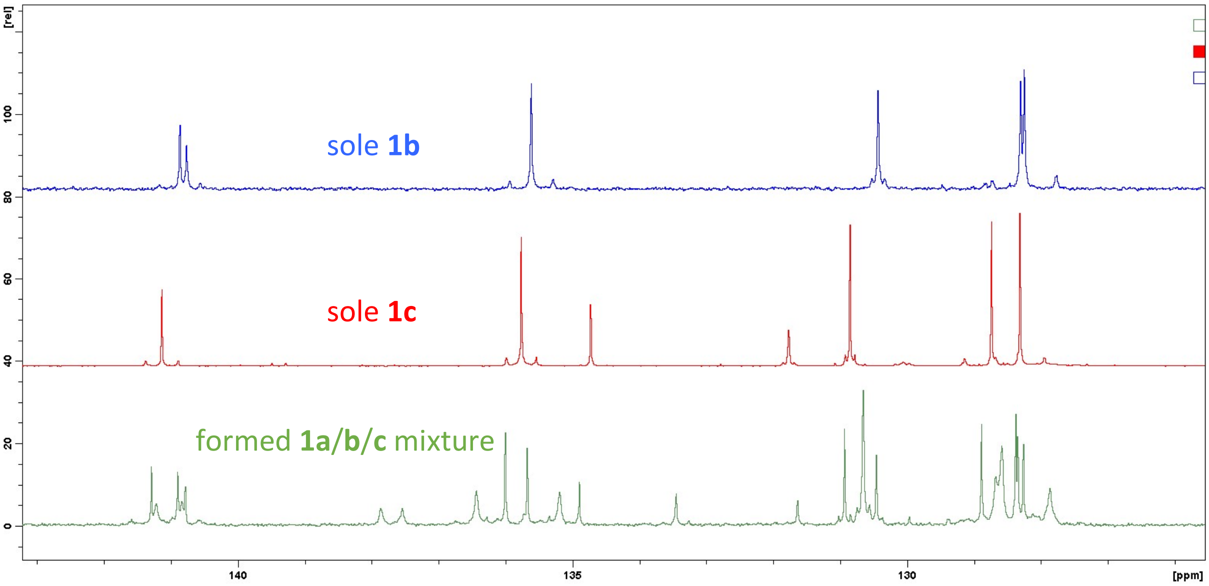

Fig. S5: Detail of the aromatic regions of the ^{13}C NMR spectra of sole **1b** (blue), **1c** (red) and **1a/b/c** mixture formed *via* the reaction of **1** with BrCN (green) measured in CDCl$_3$.

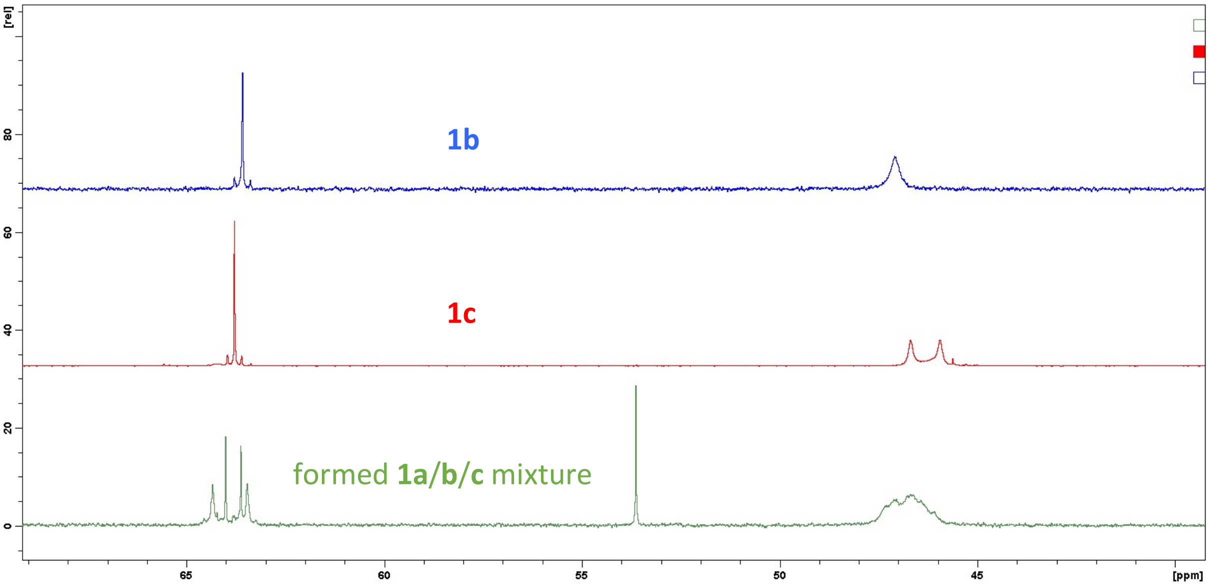

Fig. S6: Detail of the aliphatic region of the ^{13}C NMR spectra of sole **1b** (blue), **1c** (red) and **1a/b/c** mixture formed *via* the reaction of **1** with BrCN (green) measured in CDCl$_3$. The resonance at 53.6 ppm in the bottom spectrum is due to the presence of the CH$_2$Cl$_2$ solvent.

Preparation of $(L^{N})_2SnBr_2$ (2b)

2 (879 mg, 2.00 mmol) was dissolved in hexane (25 mL) and cooled down to ca. 0 °C. Solution of Br_2 (320 mg, 2.00 mmol) in cold hexane (25 mL) was then added dropwise to the hexane solution of **2**. The original dark orange reaction mixture became immediately colourless. Afterwards, filtration and evaporation of the volatiles in vacuo was carried out yielding a sticky off-white solid. The crude product was crystallized from hexane in a freezing box providing colourless crystals of **2b**. Overall yield 803 mg (67 %). M.p. > 180 °C (dec.). ^1H NMR (C_6D_6, 295 K, ppm): 0.37 (s, $Si(CH_3)_3$). $^{13}C\{^1H\}$ NMR (C_6D_6, 295 K, ppm): 5.9 ($Si(CH_3)_3$, $^1J(^{29}Si,^{13}C)$ = 57 Hz, $^3J(^{119/117}Sn,^{13}C)$ = 18 Hz). $^{119}Sn\{^1H\}$ NMR (C_6D_6, 295 K, ppm): -283.4. ^1H NMR ($CDCl_3$, 295 K, ppm): 0.37 (s, $Si(CH_3)_3$). $^{13}C\{^1H\}$ NMR ($CDCl_3$, 295 K, ppm): 5.6 ($Si(CH_3)_3$, $^3J(^{119/117}Sn,^{13}C)$ = 18 Hz). $^{119}Sn\{^1H\}$ NMR ($CDCl_3$, 295 K, ppm): -283.6. Elemental analysis (%): found C, 24.5; H, 6.2; N, 4.4. Calc. for $C_{12}H_{36}Br_2N_2Si_4Sn$ (599.28): C, 24.05; H, 6.06; N, 4.67.

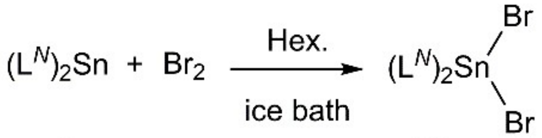

2 **2b**

Scheme S1: Exclusive preparation of **2b**

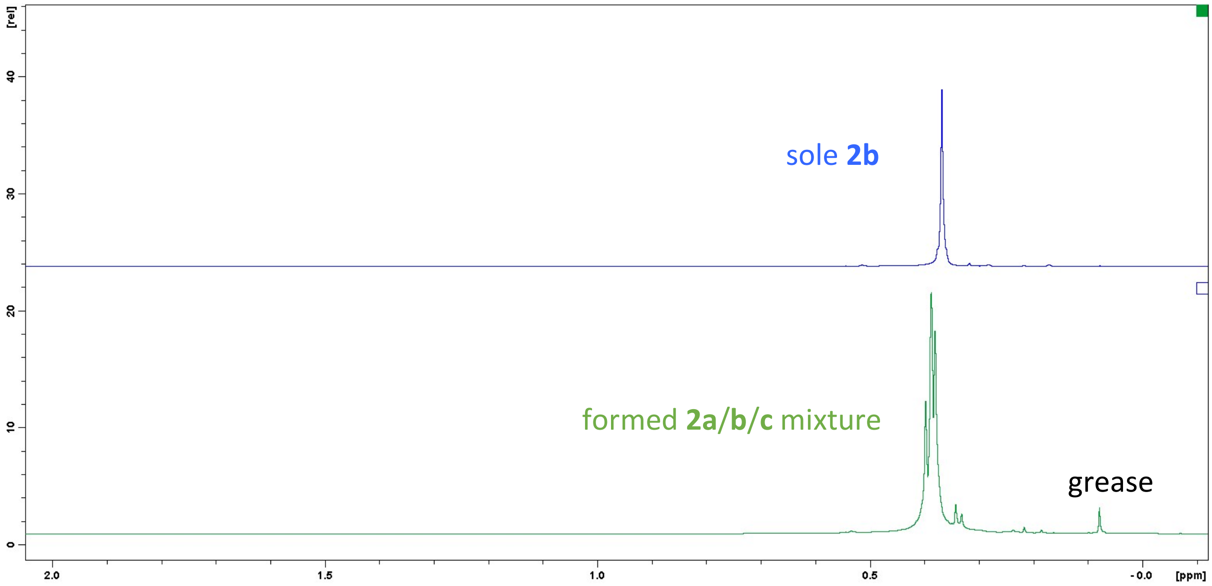

Fig. S7: ^1H NMR spectra of **2b** (blue) and **2a**/**b**/**c** mixture formed *via* the reaction of **2** with BrCN (green) measured in $CDCl_3$.

Estimation of equilibrium constants and Gibbs energies for the formation of 1a and 2a

Taking into account the NMR findings (*i.e.* the observed rough ratio of **1a**(**2a**):**1b**(**2b**):**1c**(**2c**) = 1:0.4:0.4 within the entire temperature range of 228–323 K for **1a**/**b**/**c** and 258–323 K in the case of **2a**/**b**/**c**) and stoichiometry of the reaction (*i.e.* L_2SnBr_2 + $L_2Sn(CN)_2$ = 2 $L_2Sn(Br)CN$, where L = L^{CN} or L^{N}), it is possible to at least estimate the equilibrium constant for both cases (estimation for ambient temperature of 295 K):

$$K_{c\,(295)} = \frac{[L_2Sn(Br)CN]^2}{[L_2SnBr_2][L_2Sn(CN)_2]} = \frac{1^2}{0.4 \times 0.4} = 6.25$$

Having the K_c value, determination of the ΔG_r (at 295 K) is then possible:

$$\Delta G_{r(295)} = -RTlnK_c = -8.314462 \times 295 \times ln6.25 = -4494.9\,\frac{J}{mol} \approx -1.07\,\frac{kcal}{mol}$$

The obtained ΔG_r value thus represents slightly exothermic reaction and the result are very close to ΔG_r values acquired from the theoretical calculations for the formation of both **1a** and **2a** (see the DFT calculation section in the manuscript).

Table S1: Melting points and ^{119}Sn NMR chemical shift values of prepared compounds

Compound	**M. p.**	**δ$_{solution}$ (ppm)**[a]	**δ$_{solid-state}$ (ppm)**	**c. n. (Sn)**
1a	233-234 °C[b]	-333.7	-350	6
1b	246 °C	-271.2	-290	6
1c	199-200 °C	-389.0	-394/-401	6
2a	203-205 °C (dec.)[c]	-281.8	n/a	4
2b	> 180 °C (dec.)	-283.6	n/a	4
2c	n/a	-309.7	n/a	4

[a] measured in $CDCl_3$, [b]m.p. valid for co-crystals **1a**/**b**/**c**; [c]m.p. valid for co-crystals **2a**/**b**/**c**

Table S2: Temperature dependence of the δ(^{119}Sn) of **1a**-**c** (recorded in $CDCl_3$)

Temperature [K]	δ(^{119}Sn) **1a** [ppm]	δ(^{119}Sn) **1b** [ppm]	δ(^{119}Sn) **1c** [ppm]
323	-330.9	-268.1	-386.0
308	-332.7	-270.4	-387.3
295	-333.7	-271.8	-388.0
273	-337.9	-277.0	-391.0
258	-340.1	-279.9	-392.6
243	-342.3	-282.9	-394.1
228	-344.5	-285.9	-395.5

Table S3: Temperature dependence of the δ(^{119}Sn) of **2a**-**c** (recorded in $CDCl_3$)

Temperature [K]	δ(^{119}Sn) **2a** [ppm]	δ(^{119}Sn) **2b** [ppm]	δ(^{119}Sn) **2c** [ppm]
323	-282.9	-285.4	-310.2
308	-282.4	-284.4	-310.0
295	-281.7	-283.6	-309.7
273	-281.2	-282.0	-309.3
258	-280.6	-280.8	-309.0

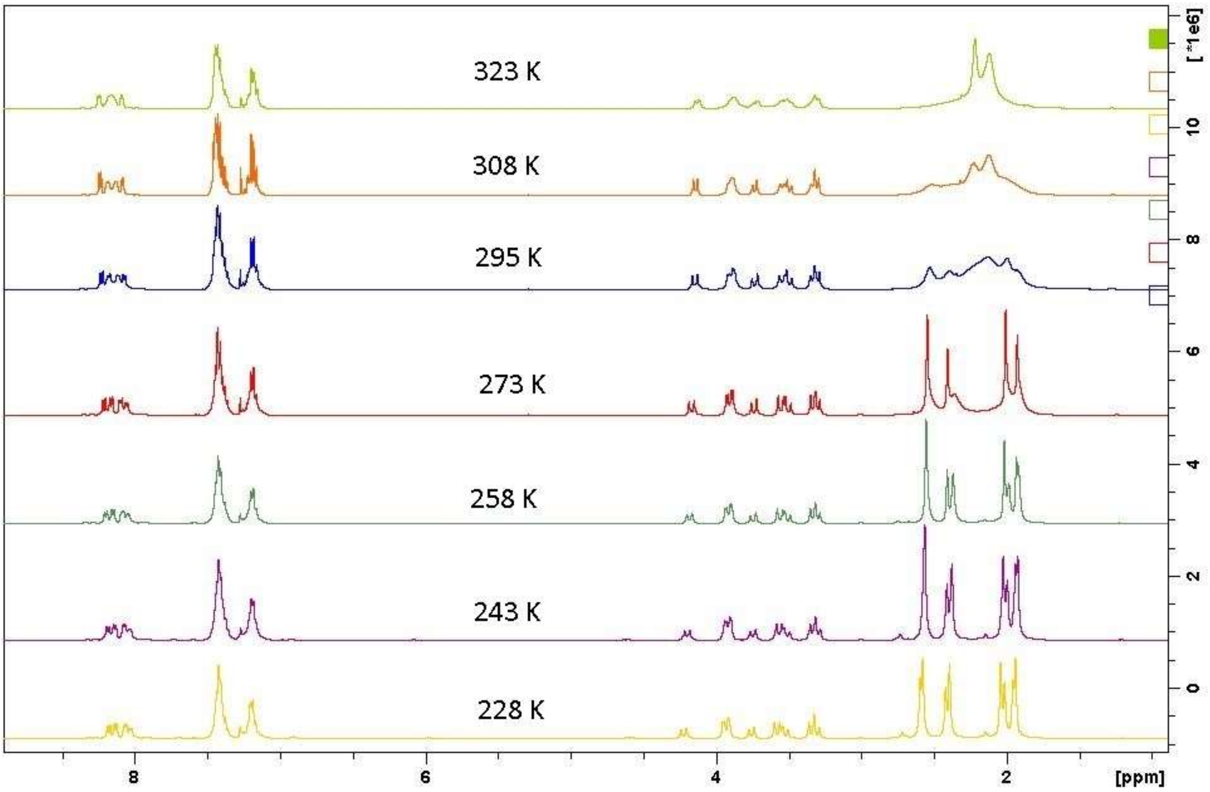

Fig. S8: ^{1}H VT NMR spectra of **1a**/**b**/**c** measured in $CDCl_3$.

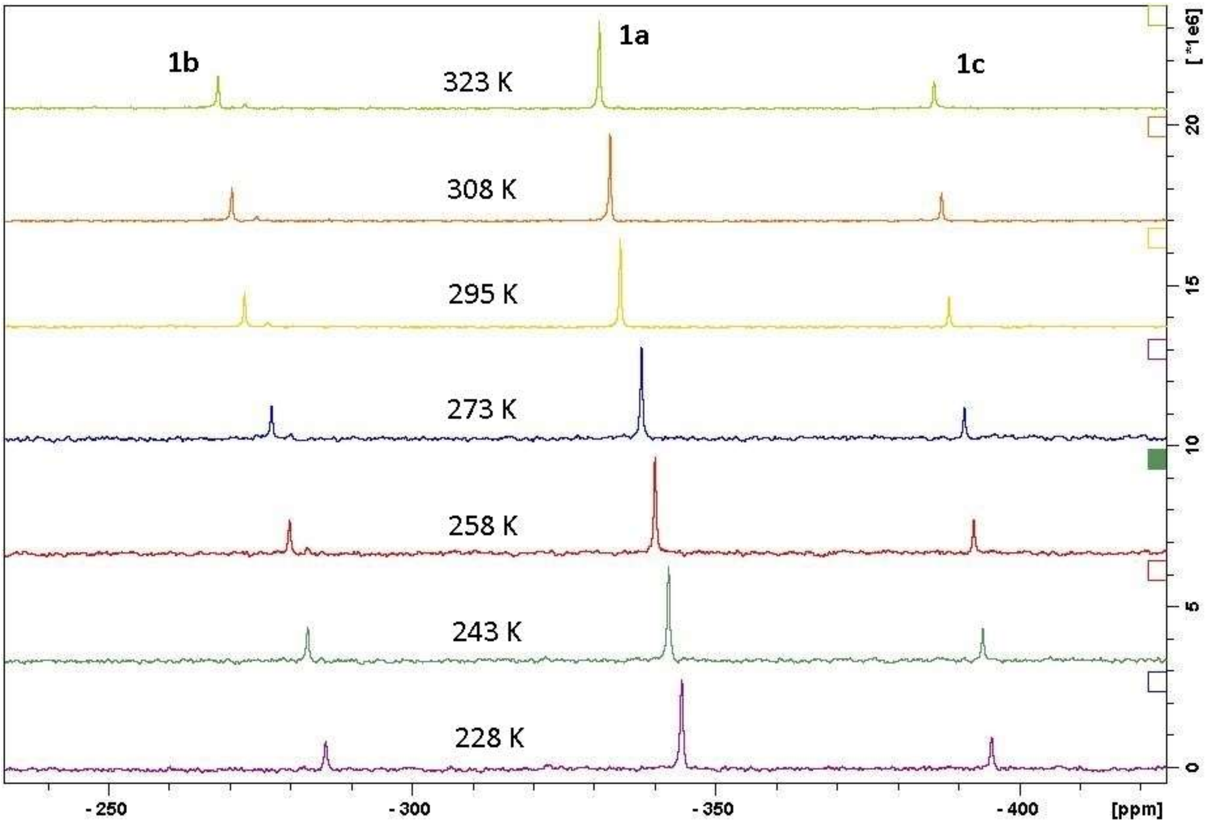

Fig. S9: ^{119}Sn VT NMR spectra of **1a**/**b**/**c** measured in $CDCl_3$.

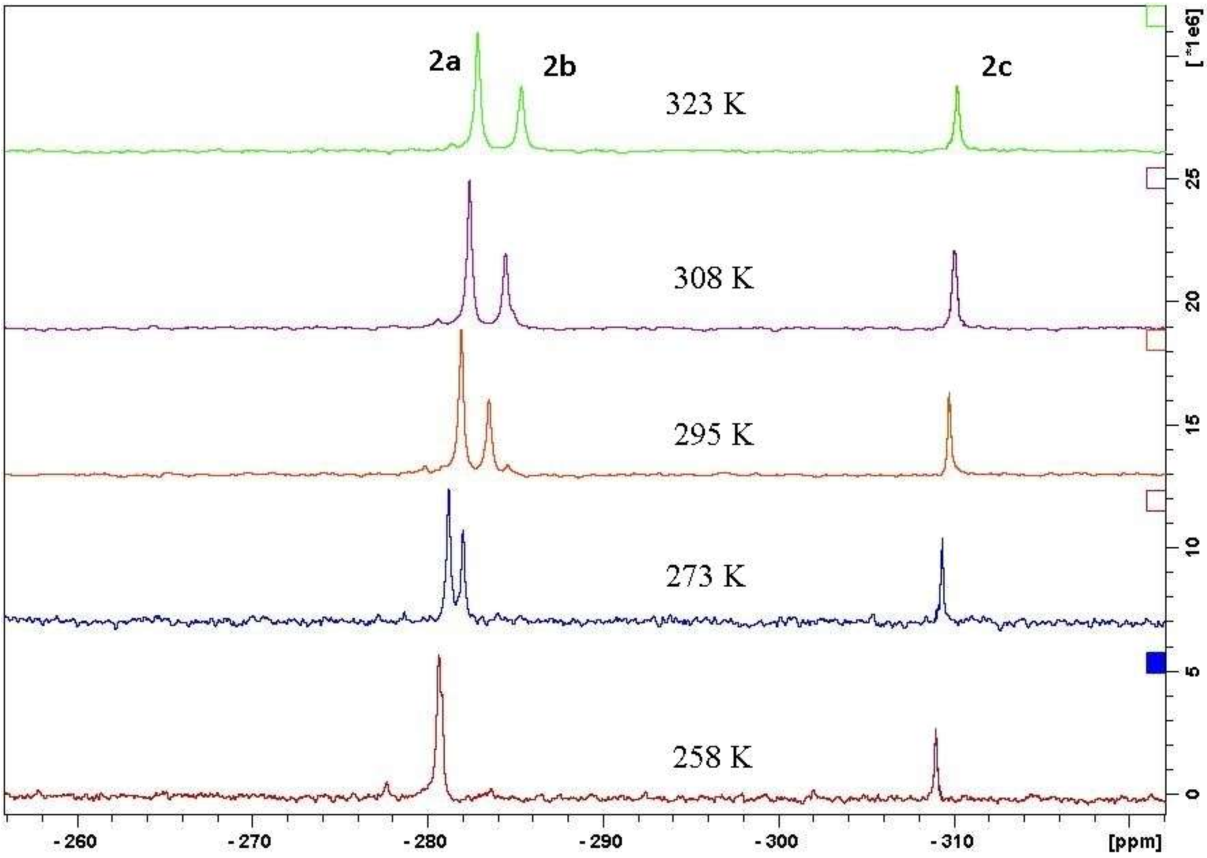

Fig. S10: ^{119}Sn VT NMR spectra of **2a**/**b**/**c** measured in $CDCl_3$. At 258 K, signals of **2a** and **2b** are overlapped by coincidence.

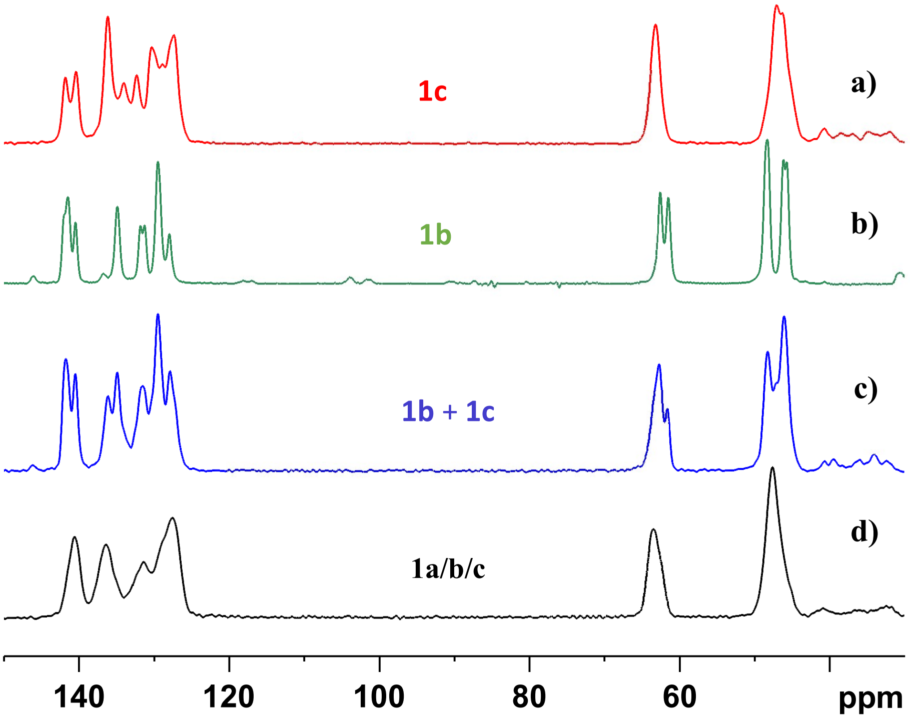

Fig. S11: ^{13}C CP/MAS NMR spectra of the investigated systems **1c** (a, red), **1b** (b, green), mechanical mixture of **1b** and **1c** (c, blue), and **1a/b/c** mixture formed *via* the reaction of **1** with BrCN (d, black).

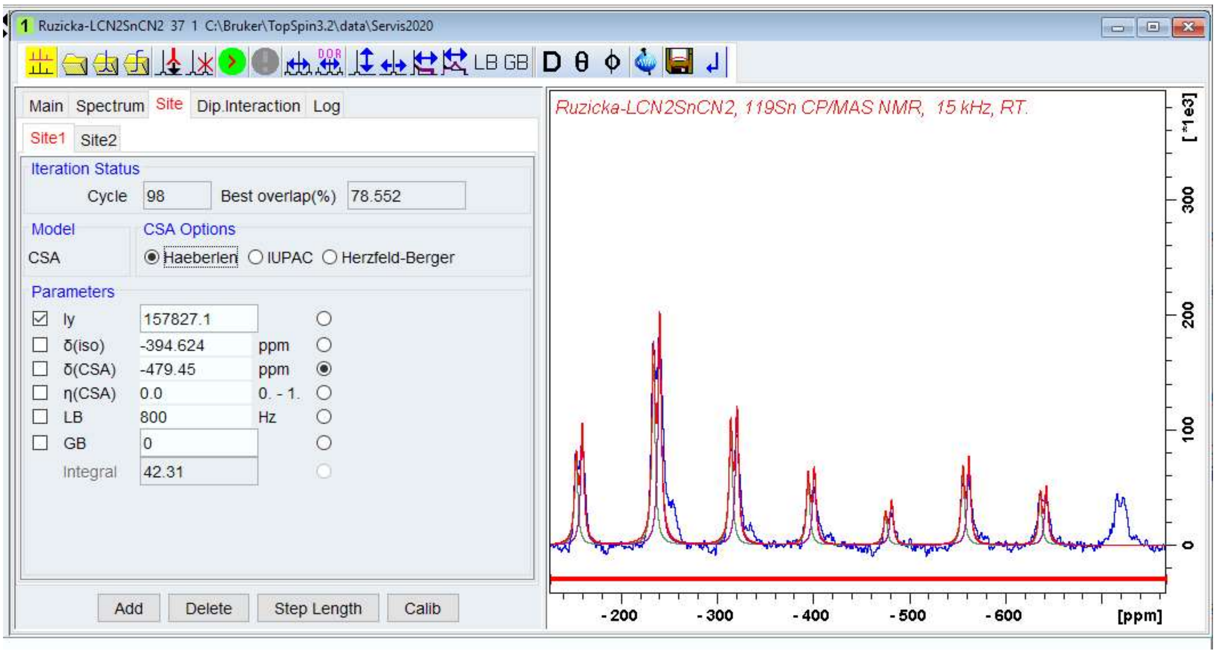

1 Ruzicka-LCN2SnCN2 37 1 C:\Bruker\TopSpin3.2\data\Servis2020

Iteration Status

Cycle 98 Best overlap(%) 78.552

Model: CSA

CSA Options: ● Haeberlen ○ IUPAC ○ Herzfeld-Berger

Parameters

☑	Iy	157827.1		○
☐	δ(iso)	-394.624	ppm	○
☐	δ(CSA)	-479.45	ppm	●
☐	η(CSA)	0.0	0. - 1.	○
☐	LB	800	Hz	○
☐	GB	0		○
	Integral	42.31		

Fig. S12: ^{119}Sn CP/MAS NMR spectrum of **1c** recorded at 15 kHz and its lineshape analysis.

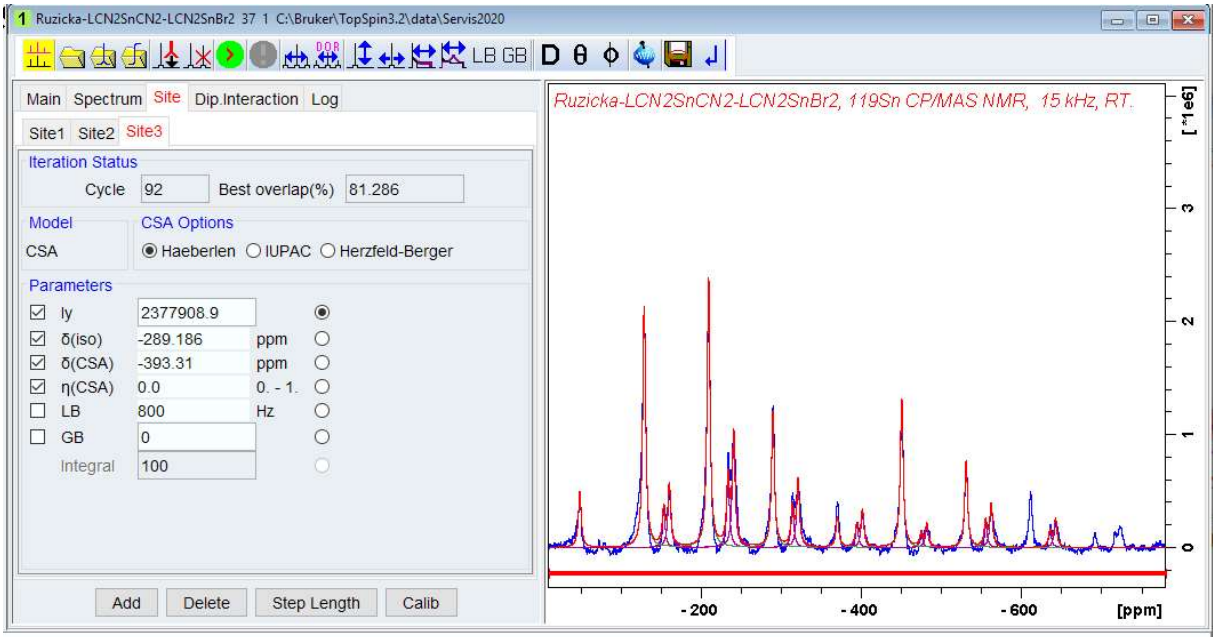

Ruzicka-LCN2SnCN2-LCN2SnBr2 37 1 C:\Bruker\TopSpin3.2\data\Servis2020

Cycle 92 Best overlap(%) 81.286

CSA ● Haeberlen ○ IUPAC ○ Herzfeld-Berger

☑ Iy 2377908.9 ●
☑ δ(iso) -289.186 ppm ○
☑ δ(CSA) -393.31 ppm ○
☑ η(CSA) 0.0 0. - 1. ○
☐ LB 800 Hz ○
☐ GB 0 ○
Integral 100

Ruzicka-LCN2SnCN2-LCN2SnBr2, 119Sn CP/MAS NMR, 15 kHz, RT.

Fig. S13: ^{119}Sn CP/MAS NMR spectrum of the mechanical mixture of **1b** and **1c** recorded at 15 kHz and its lineshape analysis.

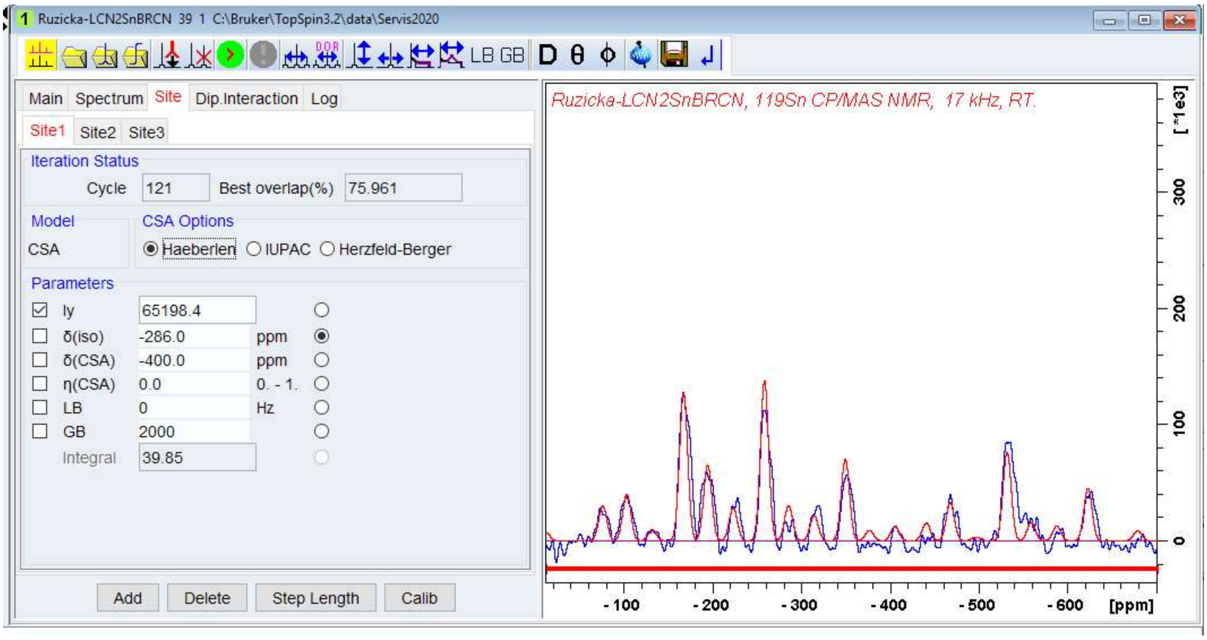

Ruzicka-LCN2SnBRCN 39 1 C:\Bruker\TopSpin3.2\data\Servis2020

Cycle 121 Best overlap(%) 75.961

CSA ● Haeberlen ○ IUPAC ○ Herzfeld-Berger

☑ Iy 65198.4 ○
☐ δ(iso) -286.0 ppm ●
☐ δ(CSA) -400.0 ppm ○
☐ η(CSA) 0.0 0. - 1. ○
☐ LB 0 Hz ○
☐ GB 2000 ○
Integral 39.85

Ruzicka-LCN2SnBRCN, 119Sn CP/MAS NMR, 17 kHz, RT.

Fig. S14: ^{119}Sn CP/MAS NMR spectrum of **1a**/**b**/**c** recorded at 17 kHz and its lineshape analysis.

Table S4: Selected crystallographic data of different solvates of **1a**

Compound	**1a**·$0.5CH_2Cl_2$	**1a**·0.5THF	**1a**·$0.17C_6H_6$
CCDC deposition number	2014595	2014599	2014597
Empirical formula	$C_{20}H_{26}BrCl_2N_3Sn$	$C_{21.20}H_{28}Br_{0.80}N_{3.20}O_{0.50}Sn$	$C_{60.11}H_{75}Br_{2.89}N_{9.11}Sn_3$
Formula weight	577.94	518.28	1512.16
Temperature/K	150(2)	150(2)	150(2)
Crystal system	Monoclinic	Triclinic	Monoclinic
Space group	Cc	P-1	C2/c
a/Å	16.2740(4)	8.4177(2)	45.2810(4)
b/Å	9.8889(3)	9.2090(3)	9.6530(3)
c/Å	14.5937(5)	15.3664(5)	29.1120(7)
α/°	90	94.2816(12)	90
β/°	103.2152(10)	90.6193(10)	107.087(3)
γ/°	90	115.8048(9)	90
Volume/$Å^3$	2286.40(12)	1068.16(6)	12163.1(5)
Z	4	2	8
ρ_{calc} g/cm^3	1.679	1.611	1.652
μ/mm^{-1}	3.109	2.706	3.167
F(000)	1144	519	6005
Crystal size/mm^3	0.413 x 0.200 x 0.200	0.374 x 0.257 x 0.117	0.414 x 0.179 x 0.117
Radiation	MoKα (λ = 0.71073)	MoKα (λ = 0.71073)	MoKα (λ = 0.71073)
2Θ range for data collection/°	2.428 to 28.000	1.330 to 28.000	1.882 to 27.499
Index ranges	-21<=h<=21, -12<=k<=13, -19<=l<=19	-10<=h<=11, -12<=k<=12, -20<=l<=20	-52<=h<=58, -12<=k<=12, -37<=l<=30
Reflections collected	13788	23476	39669
Independent reflections	5044 [R(int) = 0.0199]	5111 [R(int) = 0.0233]	13403 [R(int)=0.0517]
Data/restraints/parameters	5044 / 8 / 272	5111 / 11 / 295	13403 / 18 / 739
Goodness-of-fit on F^2	0.942	1.134	1.126
Final R indexes [I≥2σ (I)]	R1 = 0.0183, wR2 = 0.0390	R1 = 0.0201, wR2 = 0.0397	R1 = 0.0400, wR2 = 0.0700
Final R indexes [all data]	R1 = 0.0213, wR2 = 0.0396	R1 = 0.0241, wR2 = 0.0403	R1 = 0.0696, wR2 = 0.0768
Largest diff. peak/hole / e $Å^{-3}$	0.516 and -0.401	0.585 and -0.543	1.021 and -0.760

Table S5: Selected crystallographic data of **2a** and **2b**

Compound	**2a**	**2b**
CCDC deposition number	2014598	2014596
Empirical formula	$C_{12.94}H_{36}Br_{1.06}N_{2.94}Si_4Sn$	$C_{12}H_{36}Br_2N_2Si_4Sn$
Formula weight	548.50	599.30
Temperature/K	150(2)	150(2)
Crystal system	Monoclinic	Monoclinic
Space group	C2/c	C2/c
a/Å	16.8435(7)	16.6850(6)
b/Å	8.6250(3)	8.606(2)
c/Å	18.3789(8)	18.3540(11)
α/°	90	90
β/°	109.3808(15)	109.413(6)
γ/°	90	90
Volume/Å^3	2518.70(18)	2485.6(6)
Z	4	4
ρ_{calc} g/cm^3	1.446	1.601
μ/mm^{-1}	2.883	4.433
F(000)	1109	1192
Crystal size/mm^3	0.324 x 0.281 x 0.214	0.255 x 0.220 x 0.184
Radiation	MoKα (λ = 0.71073)	MoKα (λ = 0.71073)
2Θ range for data collection/°	3.841 to 27.992	2.589 to 27.498
Index ranges	-22<=h<=19, -10<=k<=11, -20<=l<=24	-21<=h<=21, -11<=k<=10, -23<=l<=21
Reflections collected	9513	8827
Independent reflections	2982 [R(int) = 0.0173]	2761 [R(int) = 0.0157]
Data/restraints/parameters	2982 / 3 / 109	2761 / 0 / 102
Goodness-of-fit on F^2	1.120	1.153
Final R indexes [I≥2σ (I)]	R1 = 0.0210, wR2 = 0.0415	R1 = 0.0176, wR2 = 0.0396
Final R indexes [all data]	R1 = 0.0255, wR2 = 0.0427	R1 = 0.0234, wR2 = 0.0413
Largest diff. peak/hole / e Å^{-3}	0.434 and -0.454	0.318 and -0.597

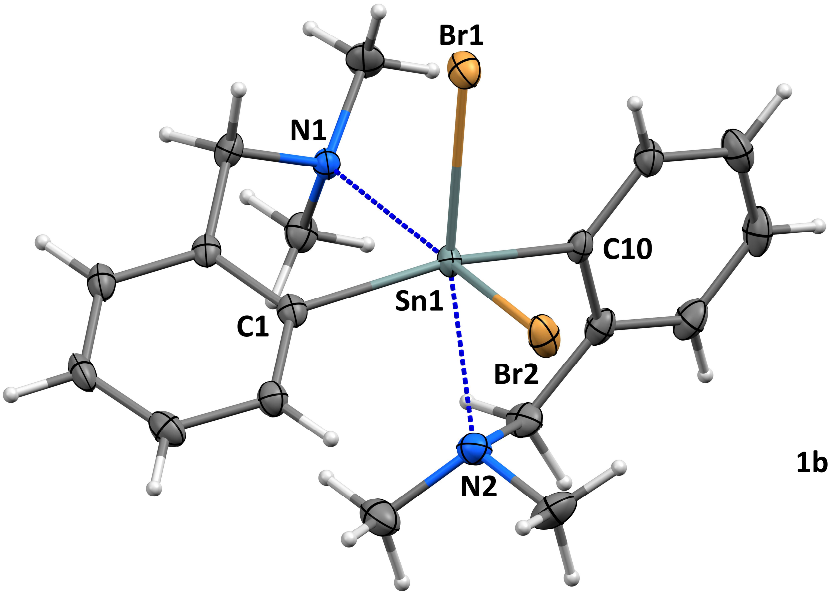

1b

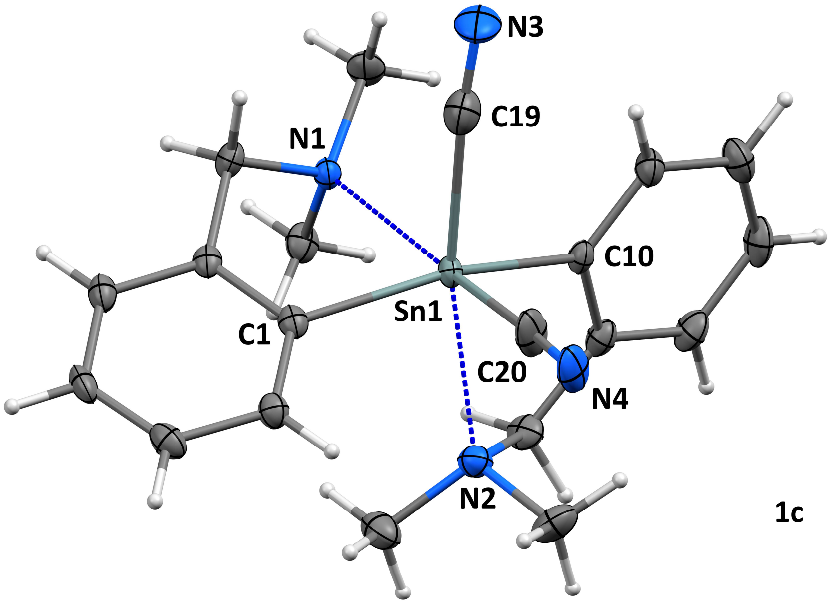

1c

Fig. S15: Molecular structures of complexes **1b**-**c** within the co-crystal of **1a**/**b**/**c**. Thermal ellipsoids are at the 40% probability level. Solvating CH_2Cl_2 molecule is omitted for clarity. Selected bond distances (Å) and angles (º): Sn1-C1 2.127(3), Sn1-C10 2.131(3), Sn1···N1 2.499(3), Sn1···N2 2.629(3), Sn1-C19 2.195(13), Sn1-C20 2.145(14), Sn1-Br1 2.655(2), Sn1-Br2 2.6523(9); C1-Sn1-C10 153.65(12), C19-Sn1-N1 82.7(6), N1-Sn1-Br2 163.17(6).

Table S6: Important bond lengths (Å) within **1a**·0.5CH_2Cl_2, **1a**·0.5THF, **1a**·0.17C_6H_6, **1b** and **1c**

Compound	**1a**·0.5CH_2Cl_2	**1a**·0.5THF	**1a**·0.17C_6H_6*	**1b**[70]	**1c**[62]
Sn···N	2.499(3) 2.629(3)	2.4818(14) 2.695(2)	2.550(3) 2.647(3) 2.580(3) 2.589(3) 2.583(3) 2.594(3)	2.581(5) 2.600(5)	2.485(3) 2.587(3)
Sn-Br	2.6523(9) 2.655(2)	2.6188(10) 2.6619(14)	2.6007(13) 2.6612(15) 2.6063(10) 2.6285(9) 2.5777(18) 2.6114(15)	2.6164(7) 2.6201(7)	
Sn-C(CN)	2.145(14) 2.195(13)	2.159(7) 2.228(7)	2.142(13) 2.207(14) 2.126(15) 2.213(18) 2.213(18) 2.265(19)		2.239(4) 2.245(5)
Sn-C(Ph)	2.127(3) 2.131(3)	2.1162(17) 2.1274(16)	2.121(4) 2.130(4) 2.126(4) 2.133(4) 2.120(4) 2.127(4)	2.114(5) 2.128 (5)	2.131(5) 2.239(4)

*The independent area contains three molecules of the complex.

[62] P. Švec, Z. Růžičková, P. Vlasák, J. Turek, F. De Proft and A. Růžička, *J. Organomet. Chem.*, 2016, **801**, 14-23.

[70] Z. Padělková, I. Císařová and A. Růžička, *Acta Cryst.*, 2005, **E61**, m2691-m2693.

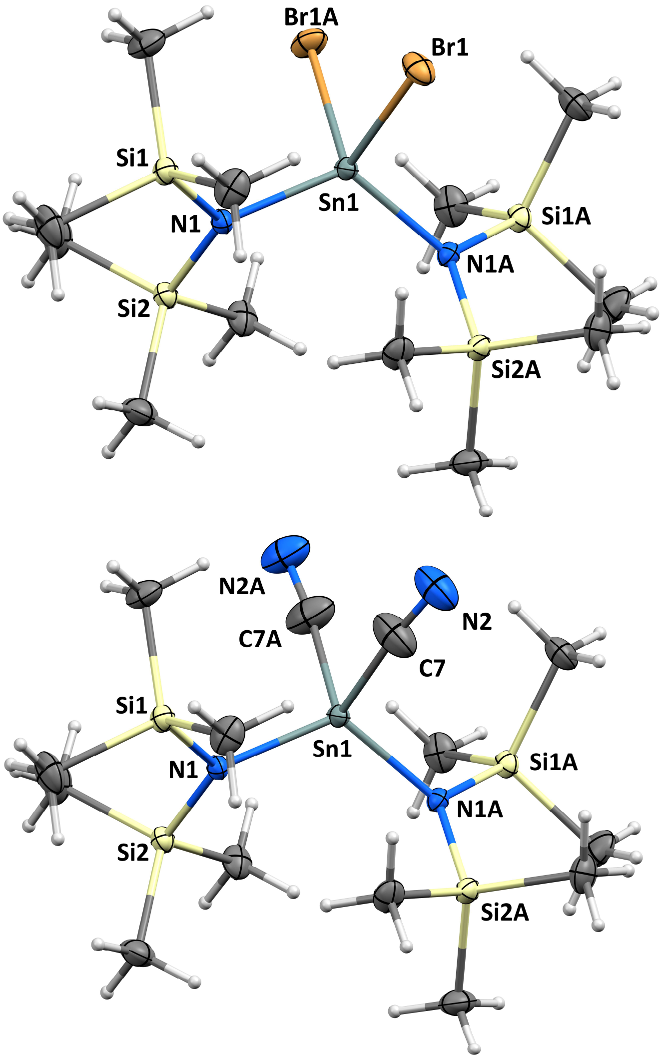

2b

2c

Fig. S16: Molecular structures of **2b**-**c**. Thermal ellipsoids are at the 40% probability level. Symmetry operations: (A) 1-x, y, 1.5-z. Selected bond distances (Å) and angles (º): Sn1-N1 2.0085(14), Sn1-C7 2.078(9), Sn1-Br1 2.5042(5); N1-Sn1-N1A 120.34(8), Br1-Sn1-Br1A 99.16(3).

Table S7: Comparison of the important bond lengths (Å) in **2a/b/c** and sole **2b**

Compound	**2b** (in **2a/b/c**)	**2b** (sole product)
Sn-N	2.0085(14)	2.0074(13)
Sn-Br	2.5042(5)	2.4754(3)

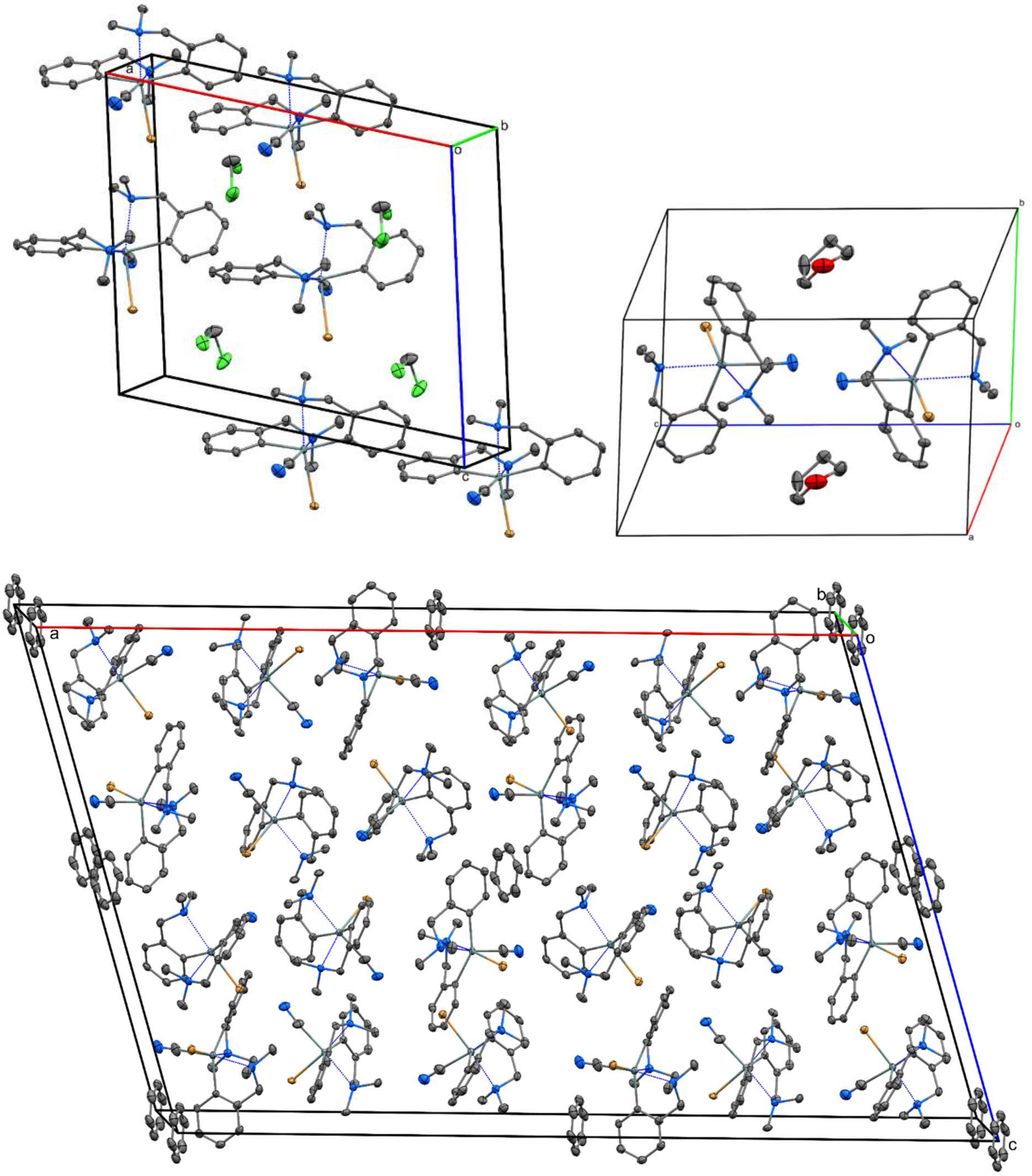

Fig. S17: Comparison of crystal packing within **1a**·$0.5CH_2Cl_2$ (upper left), **1a**·0.5THF (upper right) and **1a**·$0.17C_6H_6$ (bottom). Thermal ellipsoids are drawn at the 40% probability level. Hydrogen atoms are omitted for clarity.

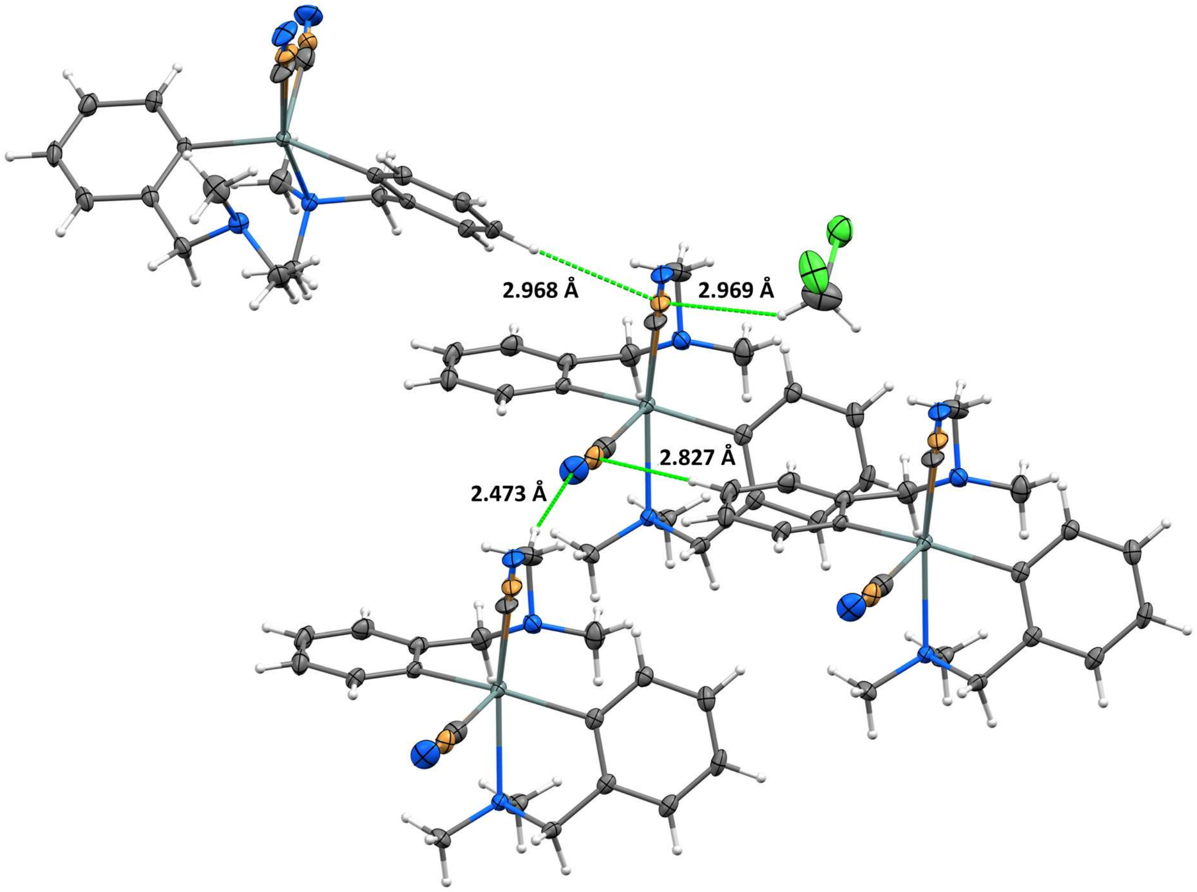

Fig. S18: Presentation of common Br···H and/or CN···H intermolecular interactions found in the co-crystal packing of **1a**/**b**/**c**·$0.5CH_2Cl_2$.

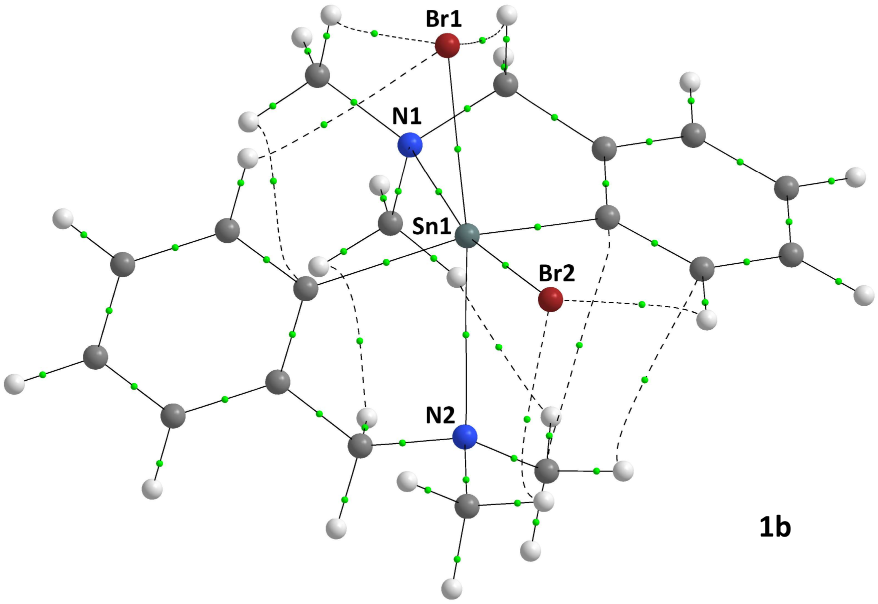

1b

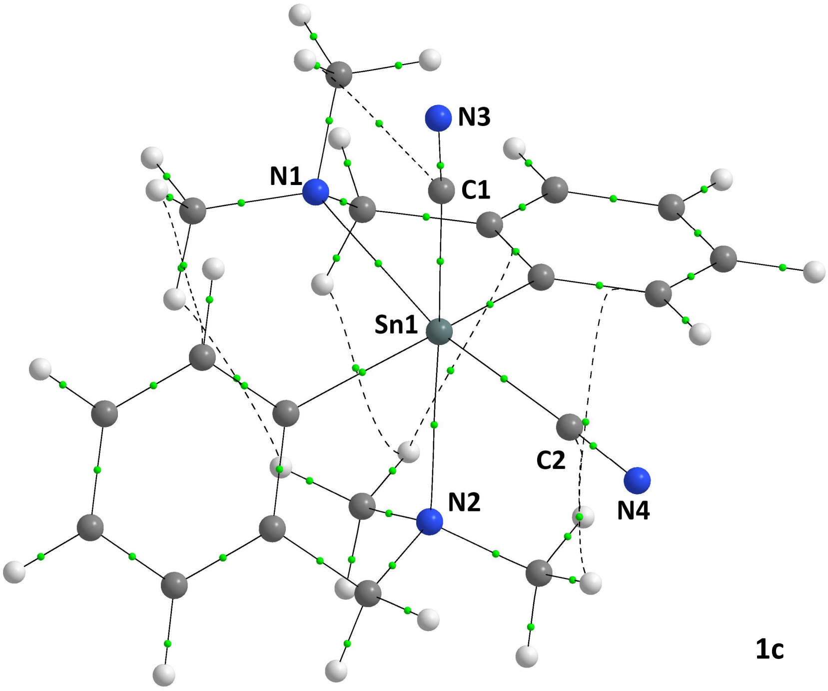

1c

Fig. S19: Theoretical molecular graphs of **1b** (top) and **1c** (bottom). Only CP(3,-1) are presented in green for clarity.

Table S8: Selected topological parameters at CP(3,-1) (a.u.) of the Sn1···N(1,2) bonds, charge on Sn and energies of Sn1···N(1,2) interactions.

Species	**Sn1 q, e**	**Bond**	**E_{int}, kcal/mol**	**$\rho(r_{cp})$**	**$\nabla^2\rho(r_{cp})$**	**$G(r_{cp})$**	**$V(r_{cp})$**	**$H(r_{cp})$**
1a	2.124	Sn1···N1	-11.62	0.038	0.105	0.032	-0.037	-0.005
		Sn1···N2	-8.37	0.031	0.084	0.024	-0.027	-0.003
1b	2.075	Sn1···N1	-10.25	0.035	0.096	0.028	-0.033	-0.004
		Sn1···N2	-8.81	0.032	0.087	0.025	-0.028	-0.003
1c	2.169	Sn1···N1	-9.43	0.033	0.091	0.026	-0.030	-0.004
		Sn1···N2	-11.14	0.037	0.103	0.031	-0.036	-0.005

*$\rho(r_{cp})$ - the electron density, $\nabla^2\rho(r_{cp})$ - the Laplacian function of the electron density, $G(r_{cp})$ - the kinetic electron energy density, $V(r_{cp})$ - the potential electron energy density, $H(r_{cp})$ - the total electron energy density. E_{int} - energies were obtained from Espinosa's equation ($E_{A\text{-}B}=1/2V(r_{cp})$). q - atomic charges from AIM.

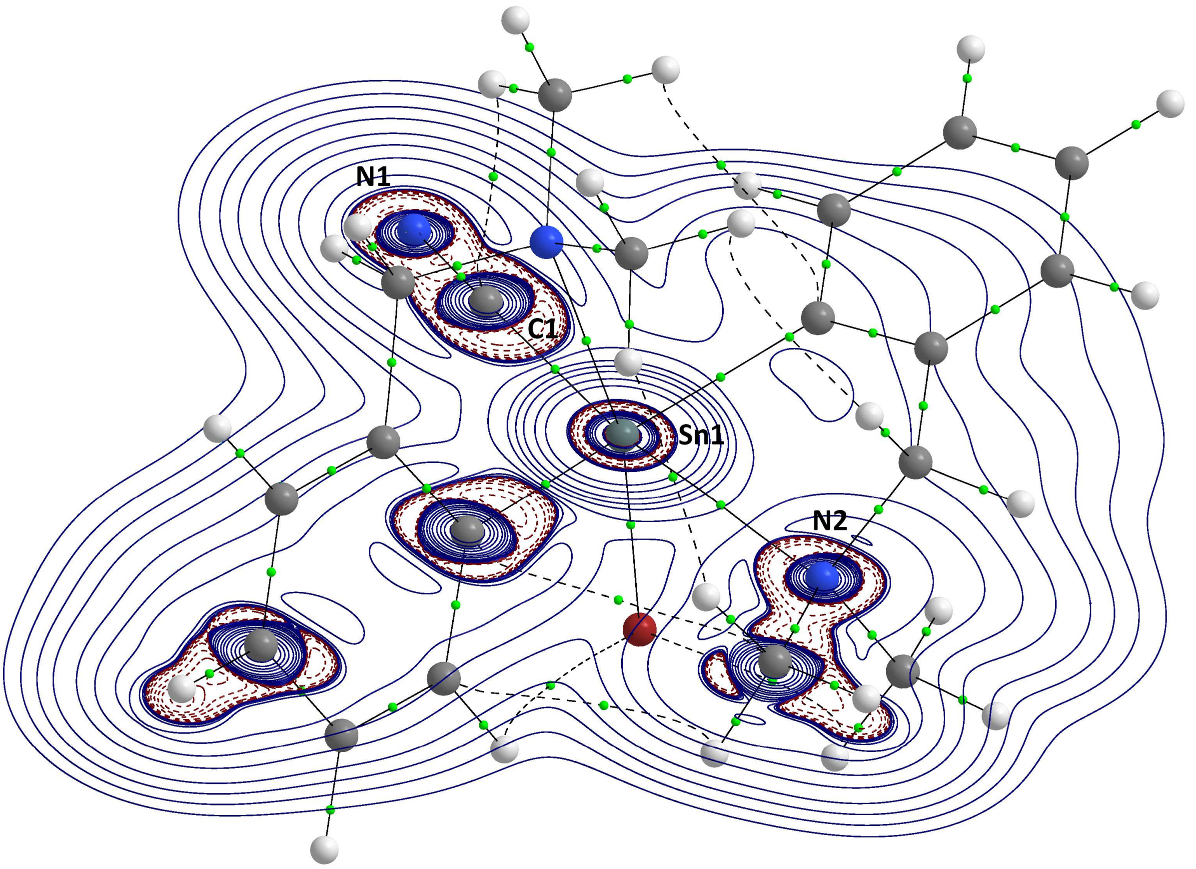

Fig. S20: Laplacian plot of the electron density distribution in C1-Sn1-N2 plane of **1a**. Red dashed lines correspond to negative values of $\nabla^2\rho(r)$, solid blue – positive. Only CP(3,-1) are presented in green for clarity.